



Proceedings of the Sixth International Conference on  
Railway Technology: Research, Development and Maintenance  
Edited by: J. Pombo  
Civil-Comp Conferences, Volume 7, Paper 13.8  
Civil-Comp Press, Edinburgh, United Kingdom, 2024  
ISSN: 2753-3239, doi: 10.4203/ccc.7.13.8  
©Civil-Comp Ltd, Edinburgh, UK, 2024

# **Performance Comparison of the Forward and Inverse Metawedge for Ground-Borne Vibration Mitigation**

**A. B. Fărăgău<sup>1</sup>, S. Van Gaal<sup>2</sup>, E. Vlijm<sup>2</sup>,  
A. V. Metrikine<sup>1</sup>, A. Tsouvalas<sup>1</sup> and K. N. van Dalen<sup>1</sup>**

**<sup>1</sup> Faculty of Civil Engineering and Geosciences, Delft University of Technology, Netherlands**

**<sup>2</sup> Cohere Consultants, Amersfoort, Netherlands**

## **Abstract**

This study examines the impact of railway-induced ground-borne vibrations on nearby structures and residents, focusing on the effectiveness of the metawedge, a novel mitigation measure. The metawedge consists of a series of periodically arranged resonators along the propagation path, either placed on the ground surface or embedded at various depths. Unlike classical locally-resonant metamaterials, the metawedge features resonators with smoothly varying resonance frequencies in the longitudinal direction. Two metawedge designs, the forward and inverse metawedge, have been proposed in the literature. Despite their similarities, they operate on different principles: the forward metawedge decelerates incoming surface waves, localizing energy, while the inverse metawedge accelerates the waves, converting Rayleigh waves into body waves. This study compares the performance of both designs in mitigating train-induced ground-borne vibrations. Results indicate that both the forward and inverse metawedge exhibit remarkably similar performance for the specific design adopted. If this similarity holds across different designs, it offers engineers flexibility in choosing the appropriate measure based on practical needs. More generally, this work demon-

strates the potential and feasibility of using metamaterials to address current and future challenges in railway transportation.

**Keywords:** ground-borne vibration, vibration mitigation, metamaterials, metawedge, railway-induced vibration, wave propagation.

## 1 Introduction

Railway transportation is increasingly favored for its considerably lower greenhouse gas emissions and its potential for complete electrification, positioning it as a highly sustainable option. However, with this surge in demand, issues that were once manageable have become substantial challenges that can disrupt regular rail operations. A prominent issue is ground-borne vibration, arising from factors like wheel and rail irregularities, the periodic excitation caused by sleepers [1, 2], and abrupt changes in track properties encountered, for example, at transition zones [2–6].

Mitigation strategies for ground-borne vibrations target various stages: at the source (e.g., vehicle-structure interactions), at the receiver (such as vibration isolating foundations), and along the transmission path. This study concentrates on the transmission path. Common mitigation methods include open or soft in-filled trenches and stiff in-filled trenches [1], which are intended to block wave propagation from the source to the receiver. The effectiveness of open or soft in-filled trenches depends on the filling material being significantly softer than the surrounding soil [7]. Experimental studies have shown that these trenches are ineffective if this condition is not met [8], requiring open trenches in soft soil environments to be quite deep, posing challenges related to depth and sidewall stability. On the other hand, stiff in-filled trenches are not subject to these constraints and have demonstrated theoretical [9] and experimental [10] effectiveness. However, their effectiveness is substantially reduced for incoming waves below a certain incidence angle [9]. This study seeks to overcome the limitations of both approaches by exploring the potential of a novel mitigation measure, the metawedge [11], to reduce ground-borne vibrations at the receiver end.

The use of metamaterials in elastic media allows for the manipulation of wave propagation, presenting innovative strategies to mitigate far-field vibrations caused by surface waves [11]. A metawedge is composed of a series of periodically arranged resonators along the longitudinal axis, each with distinct properties (see Fig. 1). This arrangement differs from traditional metamaterials as it features a progressive change in resonator characteristics. For example, the initial resonator might be positioned on the soil surface, functioning as a noise barrier, while the final one could be fully embedded [12]. Alternatively, all resonators could be placed on the ground surface with a gradual variation in natural frequencies [13]. Unlike conventional measures such as stiff in-filled trenches, the metawedge remains effective even at small incidence angles of incoming waves. Conventional metamaterials that do not feature a gradient in resonator properties, like periodic geofam-filled trenches [14] and periodic pile

barriers [15], are capable of efficiently blocking wave transmission. However, these designs tend to reflect most of the energy back towards the source. This reflection can trigger a negative feedback loop, where increased vibrations from the vehicle lead to stronger wave emissions, subsequently accelerating the degradation of railway tracks.

Two primary versions of the metawedge have been introduced in the literature [11]: the forward and inverse metawedge (see Fig. 1). In the forward metawedge, the resonator properties vary with decreasing natural frequency, whereas in the inverse metawedge, they vary with increasing natural frequency. Although these two designs share similarities, they function based on different principles: the forward metawedge decelerates incoming surface waves, concentrating energy, while the inverse metawedge accelerates the waves, transforming Rayleigh waves into body waves. Each design has its own set of practical benefits and drawbacks. This study evaluates their effectiveness in reducing train-induced ground-borne vibrations. To accomplish this, both a 2-D plane-strain model and, uniquely among most metawedge studies, a 2.5-D model are employed. The soil is modeled as a homogeneous half-space to simplify this initial analysis.

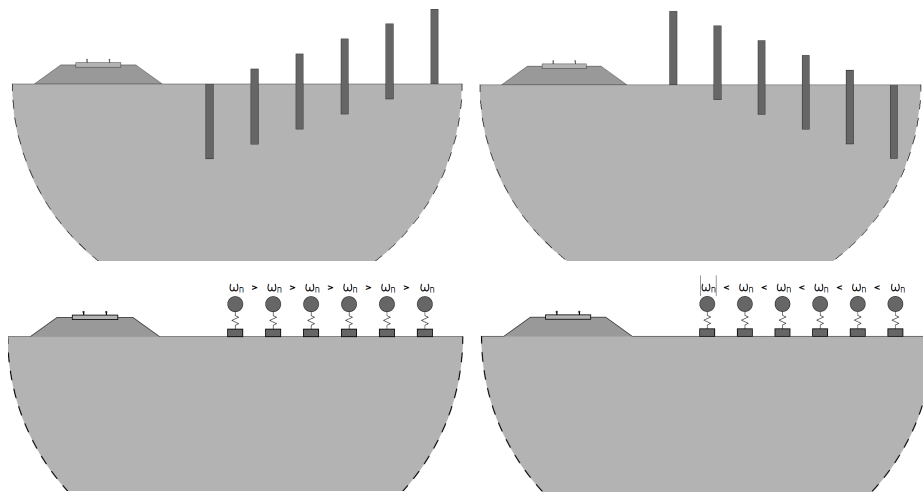


Figure 1: The two main metawedge designs (top panels): the forward (left panel) and inverse (right panel) metawedge. The surface metawedge adopted in this work equivalent to the two metawedge designs is given in the bottom panels.

The mitigation measure proposed in this work is innovative also in a broader mitigation perspective due to its potential to incorporate in its design a noise barrier (e.g., the first resonator) and integrate the advantages of the stiff trench (e.g., the last resonator being partially embedded), holding promise as a superior alternative to traditional countermeasures for both air- and ground-borne vibrations. More broadly, this study showcases the potential and feasibility of employing metamaterials to tackle present and future challenges in railway transportation.

## 2 Model formulation and the metawedge designs

### 2.1 Model formulation

To assess the metawedge's performance, this study uses two models: (i) a 2-D plane-strain model, depicted in Fig. 1, and (ii) a 2.5-D model, which is essentially a 3-D model uniform in the third direction (aligned with the train's motion). The 2-D model is employed for the initial design and evaluation of the metawedge, while the 2.5-D model examines the metawedge's effectiveness against incoming waves with different incidence angles. In both models, the soil is represented as a homogeneous half-space, and the excitation is simulated by a stationary harmonic point load at the track's location (refer to Fig. 1). Although the railway track is not explicitly modeled, its influence on the quantitative results is considered negligible for the purposes of this study.

More specifically, a unit vertical point harmonic force is exerted at a distance of 50, m from the initial unit cell of the metawedge, while the receiving point resides at the soil surface, 90 m away from the source. The soil possesses a mass density of  $\rho = 2000, \text{kg/m}^3$ , a shear wave velocity of 200 m/s, and Poisson's ratio  $\nu = 0.25$ . To accentuate the metawedge's efficacy in the absence of substantial material damping, a very slight soil damping ratio of 1, % is selected.

The response of the formulated models is obtained by using a coupled boundary-element (BE), finite-element (FE), and thin-layer (TL) methods where the resonators are modelled with FE while the soil is modelled through TL and BE. The solution method is implemented in the FEMIX software (<http://alvaroazevedo.com/femix/>) developed by de Oliveira Barbosa and his collaborators [16]. The solution method formulation is thoroughly described in Refs. [16] and its practical potential in studying ground-borne vibration in Ref. [17].

### 2.2 Metawedge designs

The process for designing the metawedge is divided into three primary stages. First, the unit cell is designed within an infinite periodic structure, ensuring one of its band gaps aligns with the target frequency range. The dispersion properties of this structure are determined using a finite element model of a general unit cell. Second, the designed unit cell is integrated into the 2-D model, incorporating a gradient in oscillator properties to identify the optimal gradient and number of cells for effective mitigation. Third, the metawedge is tested in the 2.5-D model to assess the effect of the incident angle of the incoming wave on performance. Iterations between these steps may be necessary to optimize the design.

To propose a practical and effective countermeasure, it is essential to define realistic design constraints. This study focuses on ground-borne vibrations from typical trains in the Netherlands, targeting a frequency range of 10-15 Hz. However, the metawedge design can be adjusted for other frequencies, including low frequencies

from cargo trains [12]. The design emphasizes compactness to create a structurally feasible solution with minimal urban intrusion [18]. The proposed metawedge consists of 20 resonators placed on the soil surface (see the bottom panels of Fig. 1). Surface installation is preferred for ease of construction compared to partially embedded blocks. Each resonator has a mass of 300 kg/m, with spring stiffness calibrated for natural frequencies between 10-15 Hz. In the forward metawedge, the resonator closest to the track has a natural frequency of 15 Hz, decreasing to 10 Hz for the last resonator. The inverse metawedge has a mirrored design.

The dispersion curves of a uniform metawedge (i.e., all resonators have a natural frequency  $\omega_n = 13.5 \times 2\pi$  rad/s) are presented in Fig.2. The vibration modes of the unit cell manipulate wave propagation in the medium by hybridizing with surface resonances [19]. Without the presence of resonators, the dispersion curves correspond to those of bulk and surface Rayleigh waves, represented by the straight black lines in Fig.2. However, in the presence of resonators, a band-gap is created around their natural frequency.

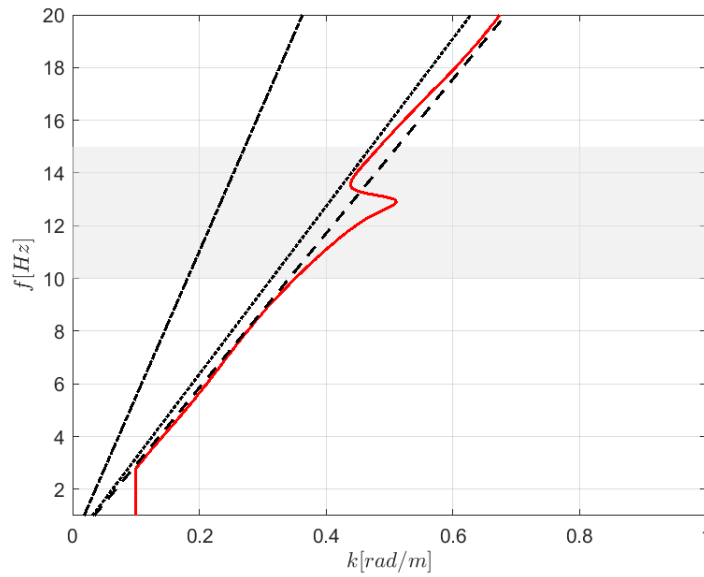


Figure 2: Dispersion curve (red line) of a uniform metawedge with resonator natural frequency  $\omega_n = 13.5 \times 2\pi$  rad/s, and dispersion curves of a homogeneous half-space: Rayleigh wave (dashed black line), shear wave (dotted black line), and compressional wave (dashed-dotted black line).

To reveal the wave manipulation properties of the two metawedge designs, Fig. 3 presents the wavenumber of a wave with frequency  $f = 23$  Hz propagating in the uniform metawedge (i.e., all resonators have the same natural frequency) versus the resonator natural frequency. This demonstrates the effect of changing the resonator natural frequency on the wave propagating through the mitigation measure. The figure shows that as the resonator natural frequency decreases from above the wave frequency (i.e.,  $f > 23$  Hz), the wave is shortened and slowed down, eventually leading

to a localization of the wave when the wave reaches the resonator with  $f = 23$  Hz; this scenario corresponds to the forward metawedge. Alternatively, as the resonator natural frequency increases from below the wave frequency (i.e.,  $f < 23$  Hz) the wave is elongated and sped up until its phase velocity surpasses the shear wave velocity at which point shear waves are excited. Essentially, surface modes with phase velocities greater than the shear-wave velocity  $c_S$  cannot exist in the elastic medium. This mechanism facilitates the transformation of surface waves into body waves that propagate deep into the ground. This scenario corresponds to the inverse metawedge.

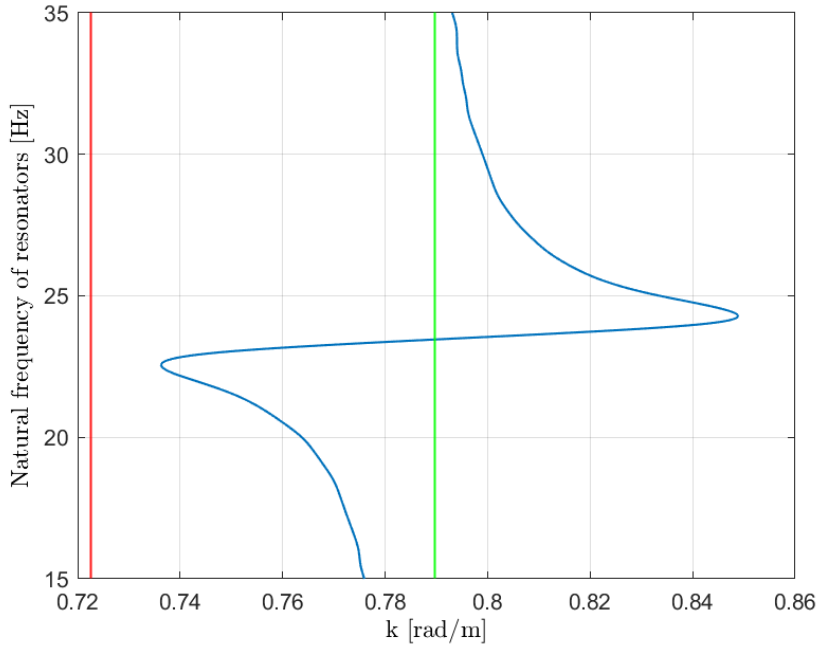


Figure 3: The wavenumber (blue line) of a wave with frequency  $f = 23$  Hz propagating in a uniform metawedge (i.e., all resonators have the same natural frequency) versus the resonator natural frequency. For comparison, the Rayleigh wavenumber (green line) and shear wavenumber (red line) corresponding to a homogeneous half-space are also presented.

### 3 Results and discussion

This section presents a performance comparison of the two metawedge designs obtained from the 2-D and 2.5-D models. The efficiency of the mitigation measures is quantified using the insertion loss  $\text{IL}_i$ , defined as the ratio of the response in the unmitigated scenario  $U_i^{\text{ref}}$  to that in the mitigated scenario  $U_i$ . This metric is expressed by the following equation [9]:

$$\text{IL}_i(x, z, \omega) = 20 \log_{10} \frac{|U_i^{\text{ref}}(x, z, \omega)|}{|U_i(x, z, \omega)|}, \quad i \in \{x, y, z\}. \quad (1)$$

### 3.1 Results from the 2-D model

The effectiveness of the designed systems in mitigating vibrations is initially evaluated in the frequency domain, assuming plane-strain conditions. In this context, the plane wave motion is perpendicular to the metawedge. Fig. 4 presents the vertical insertion loss  $IL_z$  at the soil surface and behind the mitigation measure for various excitation frequencies. This provides confirmation that both designed solutions effectively mitigate ground-borne vibration in the frequency range of 10–15 Hz, particularly for waves perpendicular to the metawedge. Interestingly, despite their different operating principles, the two designs achieve nearly identical insertion loss across the frequency range of interest.

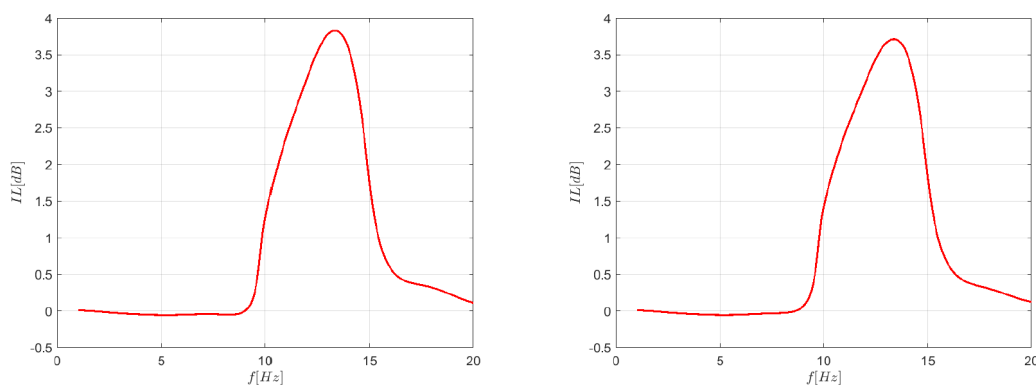


Figure 4: The vertical insertion loss  $IL_z$  at receiver position located on the soil surface behind the mitigation measure vs excitation frequency for the forward (left panel) and inverse (right panel) metawedge.

For a more comprehensive overview, Fig.5 displays the vertical insertion loss ( $IL_z$ ) across the entire spatial domain of interest for an excitation frequency of 13 Hz for both designs. While the insertion loss at the surface was nearly identical for the two designs (see Fig.4),  $IL_z$  reveals some noticeable differences with depth, despite qualitatively similar results. It is particularly evident that the inverse metawedge (bottom panel in Fig. 5) shows a more pronounced amplification deep in the ground, confirming the conversion of Rayleigh waves into bulk waves. Nevertheless, the forward metawedge, which lacks this mechanism, also exhibits amplification at this depth, albeit less pronounced. This effect is due to the inherent diffraction caused by any object positioned on the surface of the half-space, illustrating that these mitigation measures involve multiple wave manipulation and distortion mechanisms, making it challenging to isolate them even in simplified scenarios like the ones considered here.

### 3.2 Influence of wave incidence angle–2.5-D model

Given that waves generated by trains approach the countermeasure at various incidence angles, it is crucial to examine the impact of incidence angle on the metawedge's

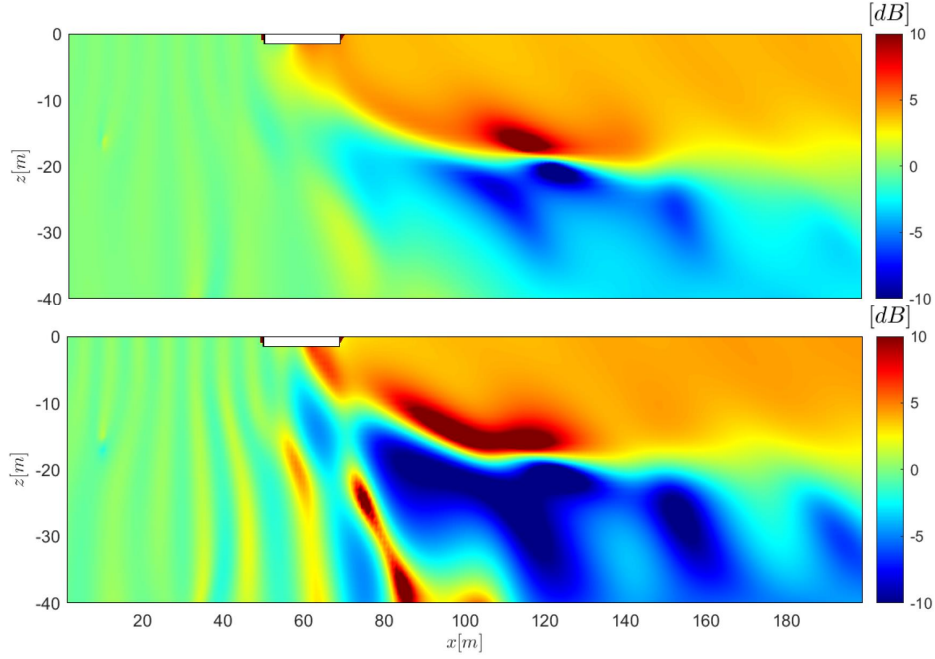


Figure 5: The vertical insertion loss  $IL_z$  in the whole spatial domain of interest for excitation frequency of 13 Hz for the forward (top panel) and inverse (bottom panel) metawedge. The white block represents the location of the metawedge.

performance. This analysis is conducted using the 2.5-D model, and thus, the insertion loss is presented in the space-wavenumber ( $k_y$  in the  $y$ -direction)-frequency domain.

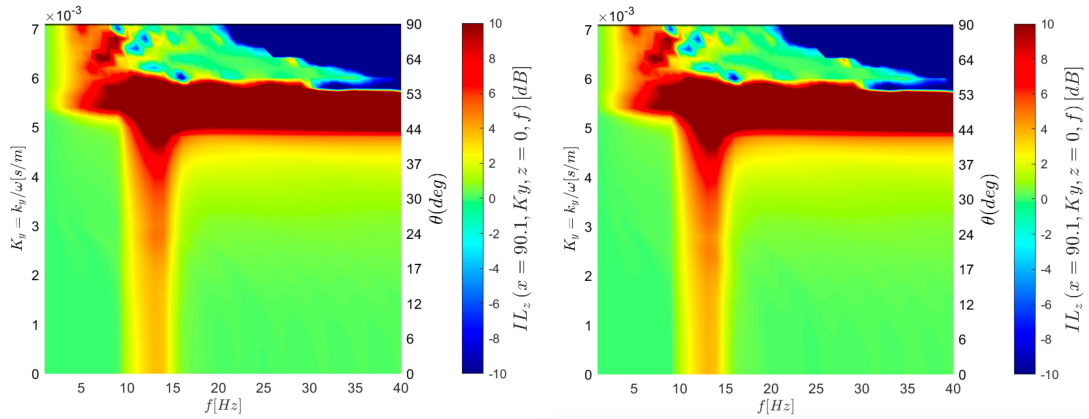


Figure 6: The vertical insertion loss  $IL_z$  vs frequency of excitation and incidence angle  $\theta$  of the incoming wave for the forward (left panel) and inverse (right panel) metawedge.

Fig. 6 shows the vertical insertion loss  $IL_z$  at a single receiver point on the soil surface behind the metawedge. The vertical axis uses  $K_y = \frac{k_y}{\omega}$  to relate wavenumber

$k_y$  to the incidence angle  $\theta$ , also indicated on the right  $y$ -axis. For small to medium angles (0–40 degrees), the metawedge is effective only for frequencies between 10–15 Hz, aligning with previous findings. Between 40–50 degrees, it is effective for frequencies above 5 Hz, likely because the oscillators are modeled as beams in the  $y$ -direction, redirecting incoming waves along the beam. At larger angles, significant amplification occurs at high frequencies, beyond the target range. Within the desired frequency range, the insertion loss remains positive for most angles.

Fig. 6 also shows that the remarkable resemblance (almost identical) insertion loss does not apply only to the waves perpendicular to the countermeasure, as seen in the previous section, but holds true for all other incident angles. However, the almost identical performance is observed only at the soil surface, as shown by Fig. 7, which presents the vertical insertion loss in all three dimensions for an excitation frequency of 13 Hz. As seen in Fig. 7, the response amplification observed deep into the ground is more pronounced in the inverse metawedge scenario, highlighting the wave-mode conversion.

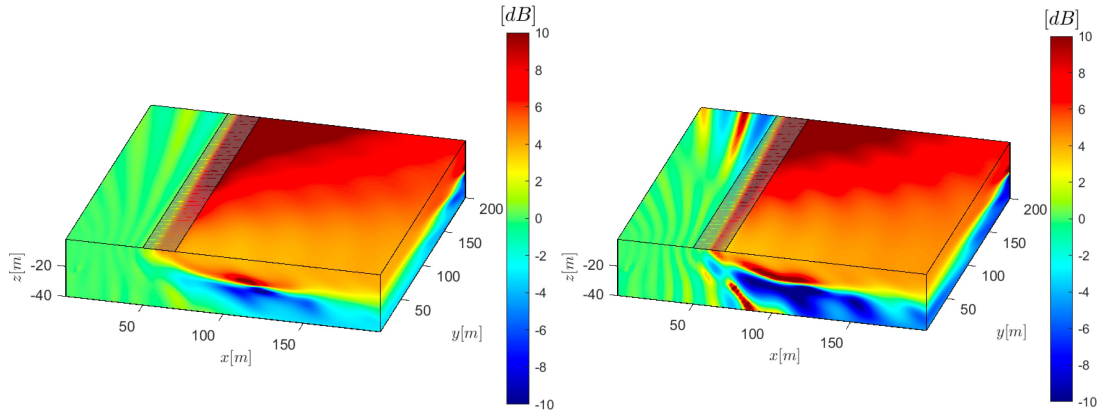


Figure 7: The vertical vertical insertion loss generated by a unit harmonic vertical point load applied at  $x = y = z = 0$  with a frequency of 13 Hz for the forward (left panel) and inverse (right panel) metawedge. The black bands indicate the position of the resonators.

Fig. 7 demonstrates the metawedge’s remarkable effectiveness in dampening vibrations along the  $x$ -axis. It performs well both within the conical region (small incident angles), where other measures fail, and beyond this region (large incident angles). This is a significant improvement over traditional trench countermeasures, which typically have limited effectiveness below a certain critical incidence angle [9].

## 4 Concluding remarks

This study examines the effectiveness of a new mitigation approach, the metawedge, in reducing railway-induced ground vibrations. It compares two designs, the forward

and inverse metawedge, which employ different mitigation mechanisms: the forward metawedge decelerates incoming surface waves, localizing energy, while the inverse metawedge accelerates waves, converting Rayleigh waves into body waves that radiate deep into the ground. A 2-D plane-strain model evaluates performance with the soil as a homogeneous half-space, and a 2.5-D model investigates the influence of incident wave angle.

Results show that both metawedge designs effectively attenuate vibrations in the 10-15 Hz frequency range typical of trains. Both designs perform similarly at the soil surface, but the inverse metawedge amplifies responses more noticeably deeper in the ground, highlighting its ability to radiate waves deeply. This similarity across designs provides engineers with flexibility in choosing the appropriate measure based on practical needs. More generally, the study demonstrates the potential and feasibility of using metamaterials to address railway transportation challenges.

## References

- [1] Geert Lombaert, Geert Degrande, Stijn François, and D. J. Thompson. Ground-Borne Vibration due to Railway Traffic: A Review of Excitation Mechanisms, Prediction Methods and Mitigation Measures. In *Noise and Vibration Mitigation for Rail Transportation Systems*, pages 253–287, 2013.
- [2] Andrei B. Fărăgău, João M. de Oliveira Barbosa, Andrei V. Metrikine, and Karel N. van Dalen. Dynamic amplification in a periodic structure with a transition zone subject to a moving load: three different phenomena. *Mathematics and Mechanics of Solids*, 27(9):1740–1760, 2022.
- [3] João Manuel de Oliveira Barbosa, Andrei B. Fărăgău, and Karel N. van Dalen. A lattice model for transition zones in ballasted railway tracks. *Journal of Sound and Vibration*, 494(November):115840, 2021.
- [4] João Manuel de Oliveira Barbosa, Andrei B. Fărăgău, Karel N. van Dalen, and Michael Steenbergen. Modelling ballast via a non-linear lattice to assess its compaction behaviour at railway transition zones. *Journal of Sound and Vibration*, 530(April):116942, 2022.
- [5] Andrei B. Fărăgău, Traian Mazilu, Andrei V. Metrikine, Tao Lu, and Karel N. van Dalen. Transition radiation in an infinite one-dimensional structure interacting with a moving oscillator—the Green’s function method. *Journal of Sound and Vibration*, 492:115804, 2021.
- [6] Andrei B. Fărăgău. *Understanding degradation mechanisms at railway transition zones using phenomenological models*. PhD thesis, Delft University of Technology, 2023.

- [7] D. J. Thompson, J. Jiang, M. G.R. Toward, M. F.M. Hussein, E. Ntotsios, A. Dijkmans, P. Coulier, G. Lombaert, and G. Degrande. Reducing railway-induced ground-borne vibration by using open trenches and soft-filled barriers. *Soil Dynamics and Earthquake Engineering*, 88:45–59, 2016.
- [8] Stijn François, Mattias Schevenels, Brian Thyssen, Jan Borgions, and Geert Degrande. Design and efficiency of a composite vibration isolating screen in soil. *Soil Dynamics and Earthquake Engineering*, 39:113–127, 2012.
- [9] P. Coulier, S. François, G. Degrande, and G. Lombaert. Subgrade stiffening next to the track as a wave impeding barrier for railway induced vibrations. *Soil Dynamics and Earthquake Engineering*, 48:119–131, 2013.
- [10] P. Coulier, V. Cuéllar, G. Degrande, and G. Lombaert. Experimental and numerical evaluation of the effectiveness of a stiff wave barrier in the soil. *Soil Dynamics and Earthquake Engineering*, 77:238–253, 2015.
- [11] Andrea Colombi, Daniel Colquitt, Philippe Roux, Sebastien Guenneau, and Richard V. Craster. A seismic metamaterial: The resonant metawedge. *Scientific Reports*, 6(Umr 7249):1–6, 2016.
- [12] Alessandro Bracci, Andrei Faragau, Andrei Metrikine, Karel Van Dalen, Roberto Corradi, and Eliam Vlijm. Assessment of the metawedge as a mitigation measure for railway induced ground vibration. In *Eurodyn Conference Proceedings*, number -, 2023.
- [13] Andrei B. Fărăgău, Sjoerd van Gaal, Eliam Vlijm, Andrei V. Metrikine, Apostolos Tsouvalas, and Karel N. van Dalen. Mitigating ground-borne vibration induced by railway traffic using metamaterials. In *30th International Congress on Sound and Vibration*, 2024.
- [14] Xingbo Pu, Zhifei Shi, and Hongjun Xiang. Feasibility of ambient vibration screening by periodic geofoam-filled trenches. *Soil Dynamics and Earthquake Engineering*, 104(July 2017):228–235, 2018.
- [15] Jiankun Huang, Wen Liu, and Zhifei Shi. Surface-wave attenuation zone of layered periodic structures and feasible application in ground vibration reduction. *Construction and Building Materials*, 141:1–11, 2017.
- [16] João Manuel de Oliveira Barbosa, Eduardo Kausel, Álvaro Azevedo, and Rui Calçada. Formulation of the boundary element method in the wavenumber-frequency domain based on the thin layer method. *Computers and Structures*, 161:1–16, 2015.
- [17] João de Oliveira Barbosa, Pedro Alves Costa, and Rui Calçada. Abatement of railway induced vibrations: Numerical comparison of trench solutions. *Engineering Analysis with Boundary Elements*, 55:122–139, 2015.

- [18] Antonio Palermo, Matteo Vitali, and Alessandro Marzani. Metabarriers with multi-mass locally resonating units for broad band Rayleigh waves attenuation. *Soil Dynamics and Earthquake Engineering*, 113:265–277, oct 2018.
- [19] Matthieu Rupin, Fabrice Lemoult, Geoffroy Lerosey, and Philippe Roux. Experimental demonstration of ordered and disordered multiresonant metamaterials for lamb waves. *Physical Review Letters*, 112(23), 2014.